
Gates are not what you need in RNNs

Ronalds Zakovskis

Ronalds.Zakovskis@lumii.lv

Andis Draguns

Andis.Draguns@lumii.lv

Eliza Gaile

Eliza.Gaile@lumii.lv

Emils Ozolins

Emils.Ozolins@lumii.lv

Karlis Freivalds

Karlis.Freivalds@lumii.lv

Institute of Mathematics and Computer Science
University of Latvia

Abstract

Recurrent neural networks have flourished in many areas. Consequently, we can see new RNN cells being developed continuously, usually by creating or using gates in a new, original way. But what if we told you that gates in RNNs are redundant? In this paper, we propose a new recurrent cell called *Residual Recurrent Unit* (RRU) which beats traditional cells and does not employ a single gate. It is based on the residual shortcut connection together with linear transformations, ReLU, and normalization. To evaluate our cell's effectiveness, we compare its performance against the widely-used GRU and LSTM cells and the recently proposed Mogrifier LSTM on several tasks including, polyphonic music modeling, language modeling, and sentiment analysis. Our experiments show that RRU outperforms the traditional gated units on most of these tasks. Also, it has better robustness to parameter selection, allowing immediate application in new tasks without much tuning. We have implemented the RRU in TensorFlow, and the code is made available at <https://github.com/LUMII-Syslab/RRU>.

1 Introduction

Recurrent neural networks (RNN) have achieved widespread use in sequence processing tasks such as language modeling and music recognition. RNNs are composed of a single computation cell, called Recurrent Unit which is unrolled along the sequence dimension.

In order to achieve stable training and the ability to store and make use of long-term dependencies, the recurrent units are designed in a special way. The most well-known units are LSTM and GRU, which use gating mechanism to store and extract information from the recurrent state. Two kinds of gates are used in these units – reset gates and update gates, where each of them is based on modulating the state information with the input information and is implemented by multiplying two values, one of which is often range-limited by the sigmoid function. Gates are considered crucial for propagation of long-term information [Greff et al., 2016] and virtually all proposals of Recurrent Units, including numerous recent developments, contain such multiplicative input-state interactions. Recent developments of improved RNN variants contain even more multiplicative interactions [Krause et al., 2016] that culminates in Mogrifier LSTM, where the input information is modulated through a series of reset gates [Melis et al., 2019]. They find that about five reset gates achieve the best performance yielding Mogrifier LSTM to be the top-performing RNN cell on several datasets so far.

In contrast, we show that gates are not essential at all to construct a well-performing recurrent unit. To this end, we develop a recurrent cell not containing a single gate. The proposed cell surpasses not only GRU and LSTM but also the so far best Mogrifier LSTM on many commonly used benchmark tasks. Our cell is based on a residual ReLU network employing normalization and ReZero [Bachlechner et al., 2020] recurrent state update.

2 Related work

A great number of RNN cells have been developed. They usually use gates to ensure stable training over many time-steps. The most well-known is LSTM [Hochreiter and Schmidhuber, 1997] which has an extra cell state that can pass information directly forward and three gates (forget, input and output) which control the data flow. This specific structure has allowed it to become the state-of-the-art cell, still being used extensively to this day. Its success is considered to stem from the 3 gates at its core, and since then, it has been considered that RNN cells need gates for optimal performance.

Following the success of the LSTM, a new cell called GRU [Cho et al., 2014] was proposed, which is loosely based on LSTM and often referred to as the light version of the LSTM. This cell combines the forget and input gates of an LSTM, resulting in 2 gates total – reset gate and update gate. As a lighter cell, it can be computed faster while the results are often similar.

Based on the marvellous results of LSTM and GRU, many extensions and modifications have been proposed. Phased LSTM [Neil et al., 2016] introduce a new time gate. Gating also in the depthwise direction is explored in Yao et al. [2015], Kalchbrenner et al. [2015]. The power of multiplicative interactions, which is the central operation in gates, is explored in Krause et al. [2016], Wu et al. [2016]. The number of gates is brought to the culmination in Mogrifier LSTM, which does input and hidden state modulation by multiple rounds of reset gates [Melis et al., 2019]. Their results suggest that using about five rounds of reset gates gives the optimal performance and positions Mogrifier LSTM as the currently best RNN cell in WikiText-2, Penn Treebank word-level and Penn Treebank character-level tasks.

Several works have questioned the necessity of the high number of gates in RNNs. Greff et al. [2016], through numerous experiments, find that the forget gate and the output activation function are the most critical components of the LSTM block and removing any of them impairs performance significantly. A similar conclusion was obtained in Van Der Westhuizen and Lasenby [2018] and a new cell called JANET was proposed, which is based on the LSTM but uses just the forget gate. The minimalistic designs of recurrent cells with only one forget gate were proposed in Zhou et al. [2016], Heck and Salem [2017]. The need for a reset gate in GRU was questioned in Ravanelli et al. [2018], where they obtain improved accuracy in Automatic Speech Recognition with the unit having only an update gate, Batch Normalization and ReLU activation.

There has been some tinkering done with using a residual shortcut connection in RNNs. Consequently, a Residual RNN [Yue et al., 2018] has been proposed. Res-RNN and gRes-RNN were proposed, where the former is a purely residual recurrent network and the latter combines residual shortcut connection with a gate. Their units show improved speed but are not able to unequivocally beat LSTM in terms of accuracy. Kim et al. [2017] proposes a Residual LSTM, which is a mix between a regular LSTM and a residual shortcut connection to improve performance in case of many layers. Even with the addition of the residual shortcut connection, it still contains a high number of gates.

3 Residual Recurrent Unit

We propose a new cell that does not contain a single gate but provides a competitive performance. We call this cell the *Residual Recurrent Unit*, RRU for short. The cell consists of a residual shortcut connection and several linear transformations employing Normalization and ReZero [Bachlechner et al., 2020] recurrent state update. ReZero is a simple zero-initialized parameter that controls how much of the residual branch contributes to the updated state. As it is initialized as 0, only the previous state is taken in effect at the first training steps, and the optimal weight for the residual branch emerges during training. Such behaviour has been shown to yield stable training for very deep ResNets and Transformers [Bachlechner et al., 2020] and here we adapt it to replace gates in recurrent networks.

The visualization of our cell can be seen in Figure 1. RRU takes input x_t at the current time-step t which is a vector of dimension m and the previous state h_{t-1} of dimension n and produces the updated state h_t and the output o_t of dimension p . The calculations done in the RRU, are described by formulas:

$$j = \text{ReLU}(\text{Normalize}(W^x x_t + W^h h_{t-1} + B^j)) \quad (1)$$

$$[j = \text{ReLU}(W^k j + B^k)]^* \quad (2)$$

$$d = \text{Dropout}(j) \quad (3)$$

$$c = W^c d + B^c \quad (4)$$

$$h_t = \sigma(S) \odot h_{t-1} + Z \odot c \quad (5)$$

$$o_t = W^o d + B^o \quad (6)$$

In the above equations, upper case letters depict the learnable parameters. Weight matrices with their respective dimensions are: $W^x - m \times g$; $W^h - n \times g$; $W^k - g \times g$; $W^o - g \times p$; $W^c - g \times n$, where g is the hidden size which we choose to be equal to $q * (m + n)$, and q is the middle layer size multiplier (we typically use values from 0.1 to 8.0). Bias vectors and their dimension are: $B^j - g$; $B^k - g$; $B^o - p$; $B^c - n$. There are two learnable scaling factors S and Z of dimension n . The sigmoid function is denoted as σ , $[\cdot]^*$ denotes the use of the equation inside the brackets zero or more times, \odot denotes scalar multiplication.

The structure of RRU is similar to the ReZero residual network [Bachlechner et al., 2020]. At first, the previous hidden state h_{t-1} and the input of the current timestep x_t are passed through a linear transformation followed by L2 normalization and ReLU. Then, zero or more linear transformations follow employing ReLU activation. Dropout [Srivastava et al., 2014] follows, and the result is linearly transformed to get two values – the output of the current timestep o_t and the hidden state candidate c . The next hidden state h_t is produced by a weighted sum of the previous state and the candidate. The candidate is scaled by a zero-initialized parameter Z according to the ReZero principle. There is a slight difference from the ReZero paper in that we use a separate scale for each feature map, but ReZero uses a common scaling factor for all maps, see Section 7 for evidence that our version works better. The scale S for the previous state is limited to the range 0 – 1 by the sigmoid function. This eliminates unstable behaviour in some cases, especially if this scaling factor becomes negative. This weight is initialized in a way that after the sigmoid, it is uniformly distributed in the range 0 – 1. This

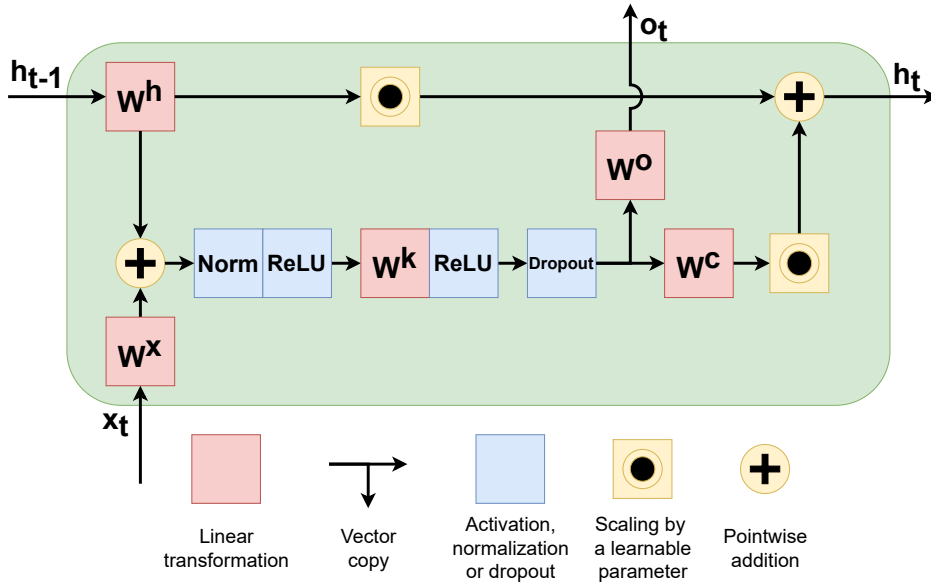


Figure 1: The structure of the *Residual Recurrent Unit* (RRU) with two state-input linear transformations.

idea is suggested by Gu et al. [2020] and relieves us from the need for another hyperparameter that needs to be tuned. We also experimented with a constant initialization of S ; that worked similarly but required an adequate constant, usually in the range 0.4 – 0.95 depending on the dataset (Section 7). Note that although Equation 5 resembles the update gate of LSTM, it is not because in the update gate, both of the multiplied values depend on the input or hidden state but in our case, S and Z are learnable parameters – effectively constants after training.

The initial hidden state h_0 is prepared to have all zeros except the first feature map, which is set to $\frac{1}{4}\sqrt{n}$. Initializing with all zeroes causes a blowup due to the employed normalization in the case when zeros are given also as the input values x_t in the first timesteps. Such inputs may occur if the input is padded by zeros from some shorter sequence.

4 Experiments

To test our unit’s performance against the chosen competitors (GRU, LSTM, Mogrifier LSTM), we run experiments on language modeling, music modeling, sentiment analysis, and MNIST image classification tasks. These tasks are commonly used for evaluating recurrent networks.

4.1 Datasets

For the polyphonic music modeling, the task is to predict the next note when knowing the previous ones. The model’s performance is measured by negative log-likelihood (NLL) loss which sums the negative logarithm of all the correct prediction probabilities. For this task, we chose four datasets that are usually evaluated together – JSB Chorales, Nottingham, MuseData, Piano-midi.de [Boulanger-Lewandowski et al., 2012]. They are already split into training, validation and testing portions. These datasets contain sequences of played piano-roll elements (MIDI note numbers between 21 and 108 inclusive), which we represent as a binary mask for each time-step, where ones are placed in the positions corresponding to the MIDI notes played at that time step. We trim or pad the sequences to length 200, similarly to how it was done by Subakan and Smaragdis [2017].

For word-level language modeling, we use the Penn Treebank dataset [Marcus et al., 1993]. The aim of this dataset is to predict the next word by knowing the previous ones. The network’s performance is measured in perplexity, which is the probability that a word will show up as the next word from the previous context. This dataset is already split into training, validation and testing portions. We use a context length of 64 and a vocabulary of 10 thousand, which includes all of the words in the dataset.

For character-level language modeling datasets we chose enwik8 [Hutter, 2012], text8¹ and Penn Treebank [Marcus et al., 1993]. The aim is to predict the next character from the previous ones. The performance is measured in BPC (bits per character), which is the number of bits used to represent a single character from the text. Penn Treebank is already split into training, validation and testing portions. However, enwik8 and text8 are not, so we use the standard split for each of them, which is 90% training, 5% validation, 5% testing. We use a window size of 512 for Penn Treebank and 256 for enwik8 and text8. The training is run in a stateful manner, meaning that we pass the old state forward to the next window (with a 10 % chance of passing a state filled with zeros). Although word-level and character-level tasks may seem similar, they evaluate different aspects of the cell. The word-level task has a large vocabulary, so the emphasis is put on evaluating RRU’s ability to deal with diverse inputs, but the character-level task has a large window size requiring the cell to remember and process long history.

The goal for IMDB sentiment analysis dataset [Maas et al., 2011] is to predict the sentiment of the text as either positive or negative. This dataset is of interest because it is quite different from the previous ones. The performance of the network is measured as the accuracy of the predictions. The challenging part of the dataset is to learn the hidden state in a way that can understand even complicated structures, for example, double negatives, etc. The dataset consists of 25 thousand training sequences and 25 thousand testing sequences. We take 5 thousand sequences from the end of the training set as a validation set. We trim the sequences to length 500 and use a vocabulary of size 10 thousand created from the most frequently occurring words (there are approximately 25 thousand different words in total) to be able to fit the sequences into our GPU memory.

¹<http://matmahoney.net/dc/textdata>

A frequently used dataset for evaluating recurrent networks is MNIST image classification. RNNs are not well suited for image classification; therefore, it puts every aspect of the network at stress. The aim here is to predict the number that each picture represents by processing a sequence that consists of all the pixels in the picture. Specifically, we use Sequential MNIST in which we take the image by pixel rows and get a single sequence and Permuted MNIST in which the pixels of each row are randomly permuted according to some fixed permutation, which makes the task harder. Each 28×28 image is transformed into a sequence of 784 elements. The dataset consists of 60 thousand training images and of 10 thousand testing images. We reserve 10 thousand images from the training data for validation.

4.2 Evaluation

For music modeling and word-level language modeling, we run hyperparameter optimization on each cell, using Bayesian hyperparameter tuning from the HyperOpt library [Bergstra et al., 2013]. The optimized hyperparameters include: number of learnable parameters, dropout rate, learning rate and some of the most influential hyperparameters specific to each cell; see Appendix A for details. The RRU cell has a built-in dropout, so to get an equitable environment, we added recurrent dropout to GRU, LSTM and Mogrifier LSTM as described by Semeniuta et al. [2016].

For character-level Penn Treebank, we also run optimization, but we only grid search through the different dropout rates from 0.0 to 0.9 – and the best testing result from these runs is shown in the results table. This experiment is further described in Section 6.

For the rest of the datasets, hyperparameter tuning would require computational power exceeding our budget, so we only run a singular experiment on each cell on as fair a configuration as possible, that is, we try to use the same configuration but sometimes changes to the configuration have to be made, for details see Appendix A.

Each experiment was done on a single machine with 16 GB RAM and a single NVIDIA T4 GPU, time spent during a single, full training varies from averagely 4 minutes (JSB Chorales) to averagely 115 hours (enwik8). We use RAdam optimizer [Liu et al., 2019] with gradient clipping. We train each dataset until the validation loss stops decreasing for 3-11 epochs, depending on the dataset.

Results of all of these experiments can be seen in Table 1. RRU is a definite leader giving the best performance on almost all of the datasets. Notably, RRU scores on top for all fully hyperparameter-optimized cases. In the two cases where RRU is outperformed, it still comes close, and it is probable that RRU would achieve the best performance if full hyperparameter optimization were performed for these datasets. Convergence graphs of some of these experiments can be seen in Appendix B.

Table 1: Evaluation results on each task. The "+/-" notation means that we did grid search through ten different dropout values to find the one which performs the best. Every metric over the horizontal line is better if it is lower and every metric under it is better if it is higher.

Task	Tuned	RRU	GRU	LSTM	Mogrifier LSTM
Music JSB Chorales (NLL)	+	7.72	8.20	8.33	8.18
Music Nottingham (NLL)	+	2.92	3.22	3.25	3.28
Music MuseData (NLL)	+	7.03	7.31	7.24	7.22
Music Piano-midi.de (NLL)	+	7.38	7.58	7.54	7.52
Word-level Penn Treebank (Perplexity)	+	102.56	122.21	140.35	126.88
Character-level Penn Treebank (BPC)	+/-	1.27	1.28	1.34	1.29
Character-level enwik8 (BPC)	-	1.37	1.53	1.49	1.36
Character-level text8 (BPC)	-	1.35	1.55	1.44	1.37
Sentiment analysis IMDB (Accuracy)	-	87.20	87.04	85.89	86.23
Sequential MNIST (Accuracy)	-	98.74	98.36	92.88	98.14
Permuted MNIST (Accuracy)	-	97.67	98.68	97.39	97.81

5 Robustness against hyperparameter choice

One of the main reasons for LSTM’s and GRU’s wide usage is their robustness against hyperparameter choice; that is, usually, you can use them with some default parameters, and they will give decent results. Such property has been described in several works, one being Talathi and Vartak [2015].

In this section, we will test the robustness for each cell to the selection of learning rate and learnable parameter count – the two most important hyperparameters. We run a grid search on Nottingham music modeling and word-level Penn Treebank language modeling datasets with a reasonably wide hyperparameter range for all the cells. We plot the validation loss and the number of epochs needed to reach the best accuracy as heatmaps in Figure 2 and 3. The figures show that our cell has a much broader range of parameters in which it works well, which also means that our cell can be used successfully without much parameter tuning. In Figure 3, we noticed that the LSTM and the Mogrifier LSTM had trouble learning anything at all on very small learning rates.

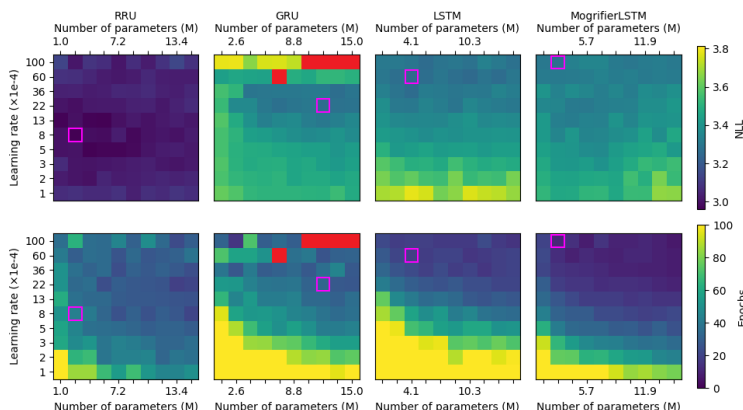


Figure 2: Robustness against learning rate and parameter count for different cells on the Nottingham dataset. The top row gives the testing NLL, and the bottom row shows the number of epochs needed to reach the best NLL. Good results are depicted with blue colour, poor results – with yellow. The red squares correspond to runs where the training failed, and the pink frames show the run with the best NLL. We observe that RRU consistently produces the best NLL across the entire range and achieves that within a small number of epochs.

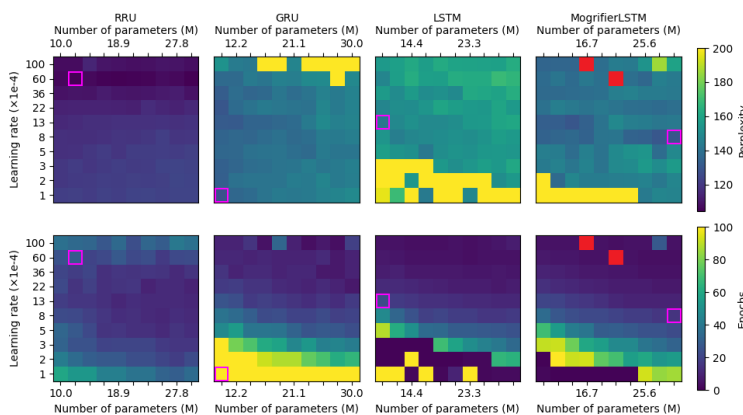


Figure 3: Robustness against learning rate and parameter count for different cells on the word-level Penn Treebank dataset. The top row gives the testing perplexity, and the bottom row shows the number of epochs needed to reach the best perplexity. Good results are depicted with blue colour, poor results – with yellow. The red squares correspond to runs where the training failed, and the pink frames show the run with the best perplexity. We observe that RRU consistently produces the best perplexity across the entire range and achieves that within a small number of epochs.

6 Dropout Analysis

While running experiments, we noticed that our cell seems to handle dropout better than the other cells. To test this observation, we ran a grid search on Nottingham and character-level Penn Treebank datasets for each cell through different dropout rates — from 0.0 to 0.9, for more details of the configurations used see Appendix A. The results from these experiments can be seen in Figures 4 and 5. From these results, we can see that all cells benefit from dropout, but for RRU, its impact is much more pronounced, and RRU ultimately reaches better final results than the other cells. We can also see that the RRU works best with a dropout rate of around 0.7. Possibly, dropout is better suited for ReLU networks, as is RRU, rather than for gated networks.

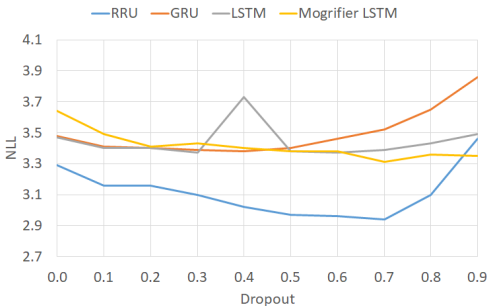


Figure 4: NLL (lower is better) depending on the dropout rate for each cell on the Nottingham dataset.

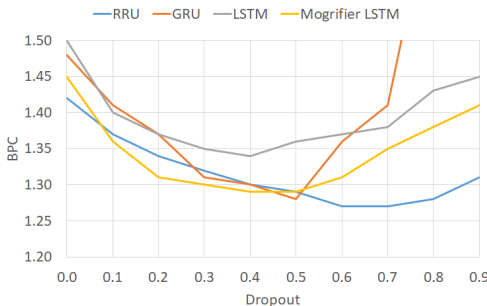


Figure 5: BPC (lower is better) depending on the dropout rate for each cell on the character-level Penn Treebank dataset.

7 Ablation study

In this section, we investigate the influence of the key elements in our cell by replacing them with simpler ones to determine whether our cell’s structure is optimal. We compare the RRU performance against versions with:

- Removed normalization.
- Using a single scalar multiplier Z for all feature maps as proposed in the ReZero paper [Bachlechner et al., 2020]. Our cell uses a different multiplier for each map.
- Added ReLU over Equations 4 and 6. Such setup is employed in some ResNet architectures [He et al., 2016b,a] and could have more expressive power.
- Residual weight S set as a constant with a scalar value 1 i.e. using an unscaled residual shortcut connection, expressing Equation 5 as $h_t = h_{t-1} + Z \odot c$.
- Residual weight S initialization with a scalar value 0.95 instead of a random one.

For these experiments, we have chosen character-level Penn Treebank, IMDB, Sequential MNIST datasets, on which we do a single run, and Nottingham, word-level Penn Treebank, on which we optimize the hyperparameters as described in Section 4. For each dataset’s configuration see the respective dataset’s configuration for RRU in Appendix A, except for character-level Penn Treebank for which the configuration differs by the dropout rate which isn’t tuned, but set as 0.3. The results can be seen in Table 2. We conclude that the current structure of our cell gives the best performance. Interestingly, the considered simplifications produce only slightly worse results, suggesting that the RRU cell’s structure is robust to changes. Although great results can be achieved without normalization, it seems to give the RRU more stability during the training and contributes to robustness (see Appendix C). We notice that our approach of using a different ReZero multiplier for each hidden map gives better performance than using only the singular scalar ReZero parameter. Adding another ReLU over the vectors c and o_t does not help. Passing the full state without a scaling factor S decreases performance. Using constant initialization seems to give similar performance, but in these experiments, the random initialization gave us better results with the added bonus of fewer hyperparameters to tune.

Table 2: Ablation study results for all of the datasets. "Character-level Penn Treebank" is denoted as "Character PTB" and "Word-level Penn Treebank" is denoted as "Word PTB" to save space.

Version	Character PTB (BPC)	IMDB (Accuracy)	Sequential MNIST (Accuracy)	Nottingham (NLL)	Word PTB (Perplexity)
RRU	1.32	87.45	98.74	2.92	102.70
no normalization	1.32	87.21	98.03	2.92	104.60
single scalar ReZero	1.32	87.08	98.45	2.97	104.44
ReLU over c and o_t	1.34	87.17	86.38	3.07	120.76
$S = 1$	2.25	86.78	98.43	3.56	110.74
S initialized with 0.95	1.33	86.71	98.60	2.96	103.09

8 Conclusion

By developing a new RNN cell without any gates and showing that it outperforms the gated cells on many tasks, we have demonstrated that gates are not necessary for RNNs. Our proposed RRU cell is robust to parameter selection and can be used in new tasks without much tuning. RRU has roughly the same speed as pure TensorFlow implementations of LSTM or GRU, and we look forward to low-level optimized CUDA RRU implementation that matches the speed of optimized LSTM and GRU implementations. We expect that the insights gained in this work will contribute to further improvements in the designs of recurrent and residual networks.

Acknowledgments and Disclosure of Funding

We would like to thank the IMCS UL Scientific Cloud for the computing power and Leo Truksāns for the technical support. This research is funded by the Latvian Council of Science, project No. lzp-2018/1-0327.

References

- T. Bachlechner, B. P. Majumder, H. H. Mao, G. W. Cottrell, and J. McAuley. Rezero is all you need: Fast convergence at large depth. [arXiv preprint arXiv:2003.04887](#), 2020.
- S. Bai, J. Z. Kolter, and V. Koltun. An empirical evaluation of generic convolutional and recurrent networks for sequence modeling. [arXiv preprint arXiv:1803.01271](#), 2018.
- J. Bergstra, D. Yamins, D. D. Cox, et al. Hyperopt: A python library for optimizing the hyperparameters of machine learning algorithms. In *Proceedings of the 12th Python in science conference*, volume 13, page 20. Citeseer, 2013.
- N. Boulanger-Lewandowski, Y. Bengio, and P. Vincent. Modeling temporal dependencies in high-dimensional sequences: Application to polyphonic music generation and transcription. [arXiv preprint arXiv:1206.6392](#), 2012.
- K. Cho, B. Van Merriënboer, C. Gulcehre, D. Bahdanau, F. Bougares, H. Schwenk, and Y. Bengio. Learning phrase representations using rnn encoder-decoder for statistical machine translation. [arXiv preprint arXiv:1406.1078](#), 2014.
- K. Greff, R. K. Srivastava, J. Koutník, B. R. Steunebrink, and J. Schmidhuber. Lstm: A search space odyssey. *IEEE transactions on neural networks and learning systems*, 28(10):2222–2232, 2016.
- A. Gu, C. Gulcehre, T. Paine, M. Hoffman, and R. Pascanu. Improving the gating mechanism of recurrent neural networks. In *International Conference on Machine Learning*, pages 3800–3809. PMLR, 2020.
- K. He, X. Zhang, S. Ren, and J. Sun. Deep residual learning for image recognition. In *Proceedings of the IEEE conference on computer vision and pattern recognition*, pages 770–778, 2016a.

- K. He, X. Zhang, S. Ren, and J. Sun. Identity mappings in deep residual networks. In European conference on computer vision, pages 630–645. Springer, 2016b.
- J. C. Heck and F. M. Salem. Simplified minimal gated unit variations for recurrent neural networks. In 2017 IEEE 60th International Midwest Symposium on Circuits and Systems (MWSCAS), pages 1593–1596. IEEE, 2017.
- S. Hochreiter and J. Schmidhuber. Long short-term memory. Neural computation, 9(8):1735–1780, 1997.
- M. Hutter. The human knowledge compression contest. URL <http://prize.hutter1.net>, 6, 2012.
- N. Kalchbrenner, I. Danihelka, and A. Graves. Grid long short-term memory. arXiv preprint arXiv:1507.01526, 2015.
- J. Kim, M. El-Khamy, and J. Lee. Residual lstm: Design of a deep recurrent architecture for distant speech recognition. arXiv preprint arXiv:1701.03360, 2017.
- B. Krause, L. Lu, I. Murray, and S. Renals. Multiplicative lstm for sequence modelling. arXiv preprint arXiv:1609.07959, 2016.
- L. Liu, H. Jiang, P. He, W. Chen, X. Liu, J. Gao, and J. Han. On the variance of the adaptive learning rate and beyond. arXiv preprint arXiv:1908.03265, 2019.
- A. Maas, R. E. Daly, P. T. Pham, D. Huang, A. Y. Ng, and C. Potts. Learning word vectors for sentiment analysis. In Proceedings of the 49th annual meeting of the association for computational linguistics: Human language technologies, pages 142–150, 2011.
- M. Marcus, B. Santorini, and M. A. Marcinkiewicz. Building a large annotated corpus of english: The penn treebank. 1993.
- G. Melis, T. Kočiský, and P. Blunsom. Mogrifier lstm. arXiv preprint arXiv:1909.01792, 2019.
- D. Neil, M. Pfeiffer, and S.-C. Liu. Phased lstm: Accelerating recurrent network training for long or event-based sequences. arXiv preprint arXiv:1610.09513, 2016.
- M. Ravanelli, P. Brakel, M. Omologo, and Y. Bengio. Light gated recurrent units for speech recognition. IEEE Transactions on Emerging Topics in Computational Intelligence, 2(2):92–102, 2018.
- S. Semeniuta, A. Severyn, and E. Barth. Recurrent dropout without memory loss. arXiv preprint arXiv:1603.05118, 2016.
- N. Srivastava, G. Hinton, A. Krizhevsky, I. Sutskever, and R. Salakhutdinov. Dropout: a simple way to prevent neural networks from overfitting. The journal of machine learning research, 15(1): 1929–1958, 2014.
- Y. C. Subakan and P. Smaragdīs. Diagonal rnns in symbolic music modeling. In 2017 IEEE Workshop on Applications of Signal Processing to Audio and Acoustics (WASPAA), pages 354–358. IEEE, 2017.
- S. S. Talathi and A. Vartak. Improving performance of recurrent neural network with relu nonlinearity. arXiv preprint arXiv:1511.03771, 2015.
- J. Van Der Westhuizen and J. Lasenby. The unreasonable effectiveness of the forget gate. arXiv preprint arXiv:1804.04849, 2018.
- Y. Wu, S. Zhang, Y. Zhang, Y. Bengio, and R. Salakhutdinov. On multiplicative integration with recurrent neural networks. arXiv preprint arXiv:1606.06630, 2016.
- K. Yao, T. Cohn, K. Vylomova, K. Duh, and C. Dyer. Depth-gated recurrent neural networks. arXiv preprint arXiv:1508.03790, 9, 2015.
- B. Yue, J. Fu, and J. Liang. Residual recurrent neural networks for learning sequential representations. Information, 9(3):56, 2018.
- G.-B. Zhou, J. Wu, C.-L. Zhang, and Z.-H. Zhou. Minimal gated unit for recurrent neural networks. International Journal of Automation and Computing, 13(3):226–234, 2016.

A Appendix A – Experiment configurations

This appendix is intended for elaboration of the configurations of the experiments that are written in Section 4.

A.1 Main experiments

All four polyphonic music datasets use the same configuration. We set context size as 200 (as done in Subakan and Smaragdis [2017]), batch size as 16, number of layers as 1, for RRU we use 1 ReLU layer and an output size of 64, all of these values we experimentally found to work well. The training stops when there hasn't been a lower NLL for 7 epochs.

For word-level Penn treebank we set context size as 64, batch size as 128, number of layers as 2, embedding size of 64, for RRU we use 1 ReLU layer and an output size of 128, all of these values we experimentally found to work well. The training stops when there hasn't been a lower perplexity for 7 epochs.

For polyphonic music modeling and word-level language modeling, we run hyperparameter optimization on each cell, where we tune the learning rate, the dropout rate and the number of parameters in 100 runs, with ranges as described in Table 3. We also tune the following parameters of the RNN cells: for RRU we tune the middle layer size multiplier q in range [0.1; 8.0]; for the LSTM we tune the forget bias in range [-3.0; 3.0]; for the Mogrifier LSTM we tune the feature rounds in range [5; 6] and the feature rank in range [40; 90], as these were mentioned as the optimal ranges in the Mogrifier LSTM paper. Optimal values for the tuned parameters for each dataset and cell can be seen in Table 4.

Table 3: Parameter ranges for main experiments that used tuning. u means the value is taken from the uniform scale and l means from the logarithmic scale. If '.' is present in the range, it means it includes float numbers, else the range is only from integers. 'M' means that the value is multiplied by 10^6 . These ranges were picked because they seemed sufficient to include all of the optimal values, which were approximately identified in the initial experiments.

Dataset	Learning rate	Dropout rate	Number of parameters
JSB Chorales			
Nottingham			
MuseData	$[1e - 4; 1e - 2]^l$	$[0.0; 0.8]^u$	$[1M - 15M]^u$
Piano-midi.de			
Word-level Penn Treebank			$[10M - 30M]^u$

For character-level Penn Treebank we set number of parameters as 24 million, learning rate as $1e - 3$, we set context size as 512, batch size as 64, number of layers as 2, embedding size of 16, for RRU we use 2 ReLU layers, middle layer size multiplier q as 4.0 and an output size of 128, for LSTM we set forget bias as 1.0, for Mogrifier LSTM we use 4 feature mask rounds of rank 24, all of these values we experimentally found to work well. The training stops when there hasn't been a lower BPC for 11 epochs. We run this configuration through ten different dropout rates from 0.0 to 0.9 and report the one with the lowest BPC.

The remaining datasets – enwik8, text8, IMDB, Sequential MNIST, P-MNIST – are run with no tuning. We tried to use the same configuration for each of the cells, but it wasn't always possible, because for some datasets some cells were unable to train with the common configuration. The configuration that was the same for each of the cells can be seen in Table 5 and the slight differences can be seen in Table 6. All of these parameter values were experimentally found to work well. enwik8 number of parameters (48 million) were taken from the Mogrifier LSTM paper and Sequential MNIST, P-MNIST number of parameters (70 thousand) were taken from Bai et al. [2018].

A.2 Robustness experiments

For Nottingham here we use the same configuration as the configuration for Nottingham in the main experiments (Section A.1), except no tuning is done, so we set middle layer size multiplier q as 2 and dropout rate as 0.5. There are 100 runs in total from a full grid search from learning rates $1e - 4$,

Table 4: Optimal values for the main experiments that used tuning. 'M' means that the value is multiplied by 10^6 . "JSB Chorales" is denoted as "JSB", "MuseData" is denoted as "Muse", "Piano-midi.de" is denoted as "Piano" and "Word-level Penn treebank" is denoted as "Word PTB" to save space.

Parameter	JSB	Nottingham	Muse	Piano	Word PTB
RRU					
Learning rate	0.00495	0.00029	0.00030	0.00077	0.00683
Dropout rate	0.79362	0.77186	0.77518	0.71577	0.66035
Number of parameters	6.9M	2.6M	8.6M	5.9M	25.9M
Middle layer size multiplier q	1.76958	7.31994	6.85699	3.68371	6.86655
GRU					
Learning rate	0.00460	0.00454	0.00260	0.00932	0.00012
Dropout rate	0.67605	0.33787	0.64839	0.75069	0.27062
Number of parameters	1.8M	3.4M	1.9M	2.4M	10.0M
LSTM					
Learning rate	0.01000	0.00882	0.00493	0.00727	0.00162
Dropout rate	0.30081	0.20310	0.35383	0.22951	0.10384
Number of parameters	1.3M	1.3M	1.8M	11.9M	14.2M
Forget bias	0.76843	-0.04104	1.85746	0.59993	-2.33114
Mogriifier LSTM					
Learning rate	0.00255	0.00169	0.00135	0.00012	0.00074
Dropout rate	0.47521	0.73808	0.55499	0.77291	0.46872
Number of parameters	1.3M	6.0M	10.3M	2.9M	24.2M
Feature mask rounds	6	5	5	5	5
Feature mask rank	58	48	76	63	74

Table 5: Parameter values for parameters that are the same for each cell in non-tuned main experiments. "Sequential MNIST", "P-MNIST" are denoted together as "MNISTs" and "text8", "enwik8" are denoted together as "wiki8s". 'M' means that the value is multiplied by 10^6 . [*RRU*] means the parameter is used in the RRU cell (same denotation is used for the other cells).

Parameter	wiki8s	IMDB	MNISTs
Number of parameters	48M	20M	70K
Context size	256	512	784
Batch size	64	64	64
Number of layers	2	2	2
Embedding size	32	64	-
Breaks after ... epochs with no performance gain	3	5	5
[<i>RRU</i>] ReLU layers	2	1	1
[<i>RRU</i>] Middle layer size multiplier q	4.0	2.0	2.0
[<i>RRU</i>] Output size	128	64	64
[<i>LSTM</i>] Forget bias	1.0	1.0	1.0
[<i>MogriifierLSTM</i>] Feature mask rounds	6	5	6
[<i>MogriifierLSTM</i>] Feature mask rank	79	40	50

Table 6: Parameters that differ between cells on some datasets in non-tuned main experiments. '*' in "Cell" field means that all cells have the same configuration.

Dataset	Cell	Learning rate	Dropout rate
enwik8	*	1e-3	0.7
text8	RRU	1e-3	0.7
	GRU	1e-4	
	LSTM	1e-3	
	Mogrifier LSTM	1e-3	
IMDB	*	1e-3	0.5
Sequential MNIST & P-MNIST	RRU	1e-3	0.7
	GRU	1e-3	0.7
	LSTM	1e-4	0.7
	Mogrifier LSTM	5e-5	0.5

$2e-4$, $3e-4$, $5e-4$, $8e-4$, $13e-4$, $22e-4$, $36e-4$, $6e-3$, $1e-2$ (ten values from $1e-4$ to $1e-2$ in logarithmic scale) – and number of parameters – 1.0M, 2.6M, 4.1M, 5.7M, 7.2M, 8.8M, 10.3M, 11.9M, 13.4M, 15.0M (ten values from 1.0M to 15.0M in uniform scale).

For word-level Penn Treebank here we use the same configuration as the configuration for word-level Penn Treebank in the main experiments (Section A.1), except no tuning is done, so we set middle layer size multiplier q as 2 and dropout rate as 0.5. There are 100 runs in total from a full grid search from learning rates – $1e-4$, $2e-4$, $3e-4$, $5e-4$, $8e-4$, $13e-4$, $22e-4$, $36e-4$, $6e-3$, $1e-2$ (ten values from $1e-4$ to $1e-2$ in logarithmic scale) – and number of parameters – 10.0M, 12.2M, 14.4M, 16.7M, 18.9M, 21.1M, 23.3M, 25.6M, 27.8M, 30.0M (ten values from 10.0M to 30.0M in uniform scale).

A.3 Dropout experiments

For Nottingham here we use the same configuration as the configuration for Nottingham in the main experiments (Section A.1), except no tuning is done, so we set the number of parameters to 5 million, learning rate as $1e-3$, middle layer size multiplier q as 2.0. We run this configuration through different dropout rates — from 0.0 to 0.9.

For character-level Penn Treebank experiment configuration see character-level Penn Treebank experiment configuration in Section A.1.

B Appendix B – Convergence speed

Convergence speed is another important factor in neural networks, for that reason, we will display convergence graphs of three datasets in this appendix, one for each training mode – JSB Chorales (tuned), character-level Penn Treebank (half-tuned) and IMDB (not tuned). The graphs are taken from the experiments done in Section 4.

Convergence graph of the JSB Chorales dataset with the best parameters found in tuning for each cell can be seen in Figure 6. We can observe that RRU in this dataset trains much faster, beating every other cell’s best NLL at 17th epoch, which implies that early stopping could be done.

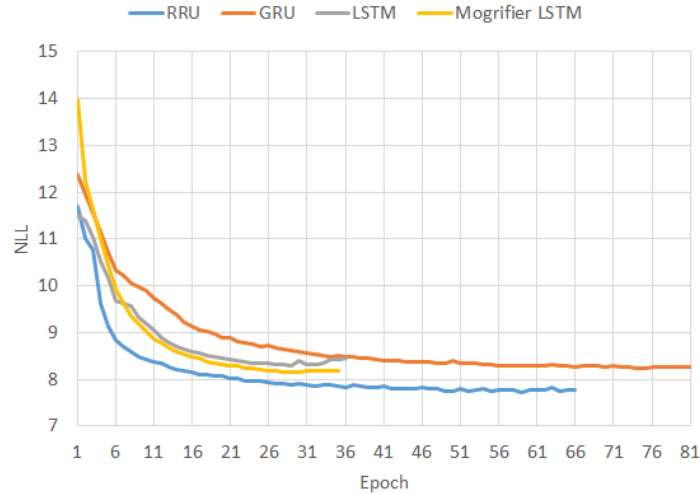


Figure 6: Validation NLL on JSB Chorales dataset for each epoch and tuned cell.

Convergence graph of the character-level Penn Treebank dataset after half-tuning (going through 10 different dropout values and taking the best one) has been done can be seen in Figure 7. We see that the RRU beats all the other cells here, while doing it in a similar epoch count as others, even when it has a larger dropout rate, which usually increases epoch count tremendously.

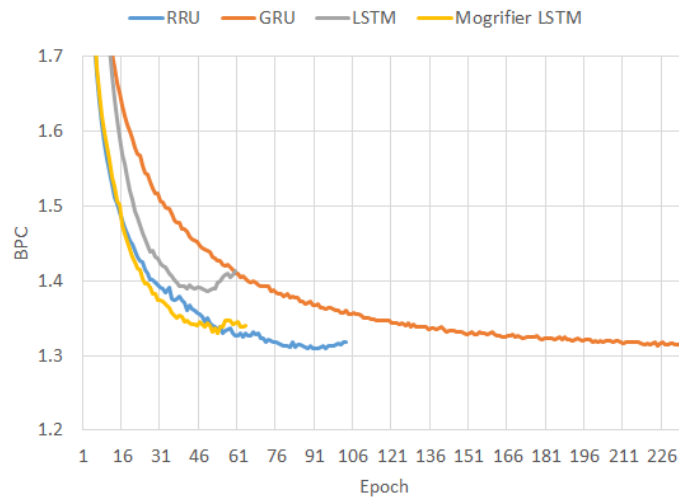


Figure 7: Validation BPC on character-level Penn Treebank dataset for each epoch and half-tuned cell. In this Figure RRU has 0.7 dropout, GRU has 0.5 dropout, LSTM has 0.4 dropout and Mogrifier LSTM has 0.5 dropout.

Convergence graph of the IMDB dataset can be seen in Figure 8. In this graph we once again see that the RRU is capable of reaching it's best accuracy first and beating the other cells with it.

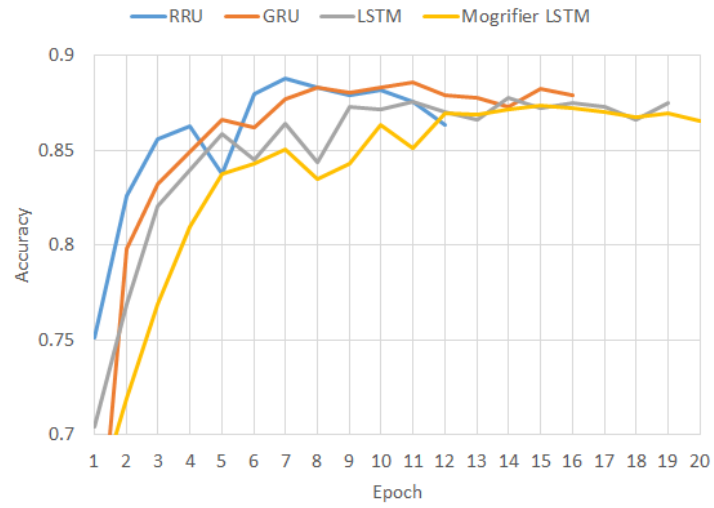


Figure 8: Validation Accuracy on the IMDB dataset for each epoch and cell.

C Appendix C – The need for normalization within the RRU

In Section 7 we looked at different RRU versions from which we concluded that our version tops the other versions, but we want to show in more detail why normalization is beneficial in the RRU. In this section, we will compare the RRU with and without normalization with the robustness tests as described in Section 5. We plot the validation loss and the number of epochs needed to reach the best accuracy as heatmaps in Figure 9. The figures show that normalization helps gain a much broader range of parameters in which it works well and helps avoid failed training sessions.

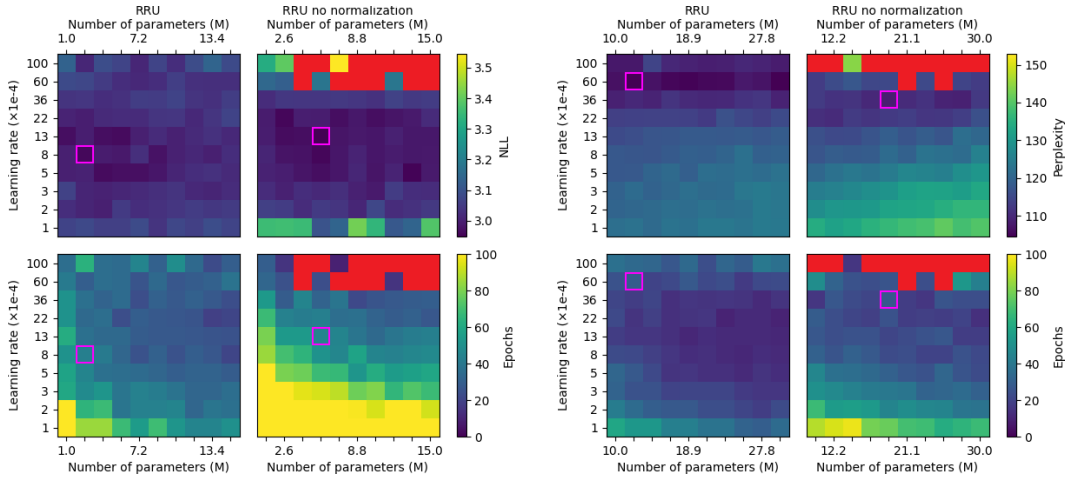


Figure 9: Robustness against learning rate and parameter count for different cells on the Nottingham (left) and word-level Penn Treebank (right) dataset. The top row gives the testing NLL (left) or perplexity (right), and the bottom row shows the number of epochs needed to reach the best loss. Good results are depicted with blue colour, poor results – with yellow. The red squares correspond to runs where the training failed by producing NaNs, and the pink frames show the run with the best NLL (left) or perplexity (right). We observe that RRU with normalization consistently produces the best loss across the entire range and achieves that within a small number of epochs.